Biochimica et Biophysica Acta 1838 (2014) 2331–2340

Contents lists available at ScienceDirect

Biochimica et Biophysica Acta

journal homepage: www.elsevier.com/locate/bbamem

Randomly organized lipids and marginally stable proteins: A coupling of weak interactions to optimize membrane signaling☆

Anne M. Rice [a,b], Ryan Mahling [a], Michael E. Fealey [a], Anika Rannikko [a], Katie Dunleavy [a], Troy Hendrickson [a], K. Jean Lohese [a], Spencer Kruggel [a], Hillary Heiling [a], Daniel Harren [a], R. Bryan Sutton [b], John Pastor [c], Anne Hinderliter [a,*]

[a] Department of Chemistry and Biochemistry, University of Minnesota Duluth, Duluth, MN, USA
[b] Department of Cell Physiology and Molecular Biophysics, Texas Tech University Health Sciences Center, Lubbock, TX, USA
[c] Department of Biology, University of Minnesota Duluth, Duluth, MN, USA

ARTICLE INFO

Article history:
Received 6 December 2013
Received in revised form 28 February 2014
Accepted 14 March 2014
Available online 21 March 2014

Keywords:
C2 domain
Disorder
Signaling
Membrane domain
Information theory

ABSTRACT

Eukaryotic lipids in a bilayer are dominated by weak cooperative interactions. These interactions impart highly dynamic and pliable properties to the membrane. C2 domain-containing proteins in the membrane also interact weakly and cooperatively giving rise to a high degree of conformational plasticity. We propose that this feature of weak energetics and plasticity shared by lipids and C2 domain-containing proteins enhance a cell's ability to transduce information across the membrane. We explored this hypothesis using information theory to assess the information storage capacity of model and mast cell membranes, as well as differential scanning calorimetry, carboxyfluorescein release assays, and tryptophan fluorescence to assess protein and membrane stability. The distribution of lipids in mast cell membranes encoded 5.6–5.8 bits of information. More information resided in the acyl chains than the head groups and in the inner leaflet of the plasma membrane than the outer leaflet. When the lipid composition and information content of model membranes were varied, the associated C2 domains underwent large changes in stability and denaturation profile. The C2 domain-containing proteins are therefore acutely sensitive to the composition and information content of their associated lipids. Together, these findings suggest that the maximum flow of signaling information through the membrane and into the cell is optimized by the cooperation of near-random distributions of membrane lipids and proteins. This article is part of a Special Issue entitled: Interfacially Active Peptides and Proteins. Guest Editors: William C. Wimley and Kalina Hristova.

1. Introduction

A cell membrane is a pliable and responsive surface. Changes in the local environment of a given lipid are propagated in all directions within a leaflet by the weak cooperative interactions between each lipid molecule and its six nearest neighbors [1]. This type of propagation behavior suggests that the membrane has great signaling potential. Another key facet to consider with regard to biological membranes and signaling is the high degree of lipid species diversity. The distribution and diversity of lipids in eukaryotic membranes are thought to maintain the system in a nearly random distribution which, according to information theory [2], maximizes the amount of information that can be cooperatively propagated in a signaling event because it is not biased in any one direction as in a more ordered system. Together the weak cooperativity of lipid molecules and their nearly random distribution suggest that the membrane constitutes a major information transducer in the cell.

To transduce the vast array of information encoded within the mosaic membrane into the cell interior requires both transient organization of the signaling lipid species and a recipient protein that further senses and propagates the message. A lipid mixture near a critical point, teetering on a phase boundary between random distribution and a restricted domain, could fulfill the first requirement. Domain formation can increase the probability of a particular signaling event for instance, by providing platforms for protein–protein interactions that initiate the intracellular portion of a signaling cascade. In this sense, transient order in lipid organization allows for a discrete message to be propagated at levels above background thermal noise, or in other words, above the milieu of all other possible messages encoded in the membrane lipid distribution.

Subsequent detection and propagation of such a wide range of membrane-encoded messages would seem to require a protein with complementary features; the protein would need to have a tendency towards random distributions so as to maximize the amount and diversity of information that can be recognized and propagated. Intrinsically

☆ This article is part of a Special Issue entitled: Interfacially Active Peptides and Proteins. Guest Editors: William C. Wimley and Kalina Hristova.

* Corresponding author at: University of Minnesota Duluth, 1039 University Dr., Duluth, MN 55812, USA. Tel.: +1 218 726 7062; fax: +1 218 726 7394.
E-mail address: ahinderl@d.umn.edu (A. Hinderliter).

http://dx.doi.org/10.1016/j.bbamem.2014.03.005
0005-2736/

disordered proteins are one well-known class of proteins with this tendency. Intrinsically disordered proteins are natively unfolded and have significant structural and conformational plasticity making them uniquely sensitive to differences in the local environment, not unlike the near random but pliable membrane surface. Moreover, intrinsic disorder can facilitate propagation of information within the body of a protein [3]. When we measured the stability of a specific class of proteins by thermal denaturation we found that these proteins, whose functional role is directly linked to membrane biology, have features of intrinsic disorder; these proteins retain some secondary structure, but are marginally stable (hypostable) or nearly disordered [4–6]. Specifically, this seems to be the case with C2 domains of synaptotagmin I (Syt I) in neurons (involved in exocytosis) and the C2 domains of dysferlin (Dys) in muscle (responsible for sensing and repairing membrane damage). Currently there are 14,496 C2 domains annotated in 9,258 protein sequences within the SMART non-redundant database [7]. It is unknown if this marginally stable behavior is a general feature of C2 domains but denaturations carried out previously on various C2 domains from protein kinase C also converge on this finding [8]. Moreover, when we denatured the C2A domain of cotton Syt I, we found it had the same hallmarks as human Syt I, suggesting potential conservation across phylogenetic kingdoms.

A new potential rule for membrane signaling emerges when we simultaneously consider the near disordered nature of membrane lipids and membrane-sensing proteins, namely the maximum flow of signaling information through the membrane and into the cell is optimized by cooperation of the two near-random distributions of membrane lipids and proteins. Indeed, when lipid species diversity and protein intrinsic disorder are compared, both increase with organism complexity [9,10]. While at first glance, this hypothesis may seem to imply unidirectionality of information flow (a marginally stable protein only decodes the information of the membrane), the mechanism applies in both directions. Protein interactions with membranes can induce membrane domain formation (order) if the protein has specificity for some of the lipids and these lipids are distributed non-ideally [11,12]. If, however, the protein's interaction with a membrane depends on intracellular signals (such as calcium ion), then the protein becomes a means to relay intracellular conditions back to the membrane potentially for amplification *via* weak cooperative lipid–lipid interactions. The end result is a reciprocal exchange of information.

Here we explore our hypothesis that the distribution of lipids within the eukaryotic membrane is coupled to interactions with weakly stable but structured proteins to transduce and modulate signaling information. We first use experimental data from the literature on membrane phospholipid compositions in stimulated and unstimulated mast cells to calculate information content encoded within different lipid compositions (excluding cholesterol as a component) as well as their associated acyl chains and head groups [13]. We then complement these findings with recent and new measurements of protein stability and membrane disruption in which membrane lipid composition (and thus information content) is a variable. We find that C2 domain stabilities are highly sensitive to lipid compositions and undergo correlated changes with membrane information content.

2. Materials and methods

2.1. Protein constructs

The C2 domains studied were constructs derived from human Syt I, cotton Syt I, and Dys. The only C2A construct of human Syt I used for experiments in this study contained residues 96–265. In the top half of Table 3, thermodynamic parameters are reported for a shorter human Syt I C2A construct containing residues 140–265. Additional residues in the 96–265 C2A construct correspond to the region between C2A and Syt I's single transmembrane helix. The human Syt I C2B domain included residues 272–422. The constructs from Dys include two different isoforms of the C2A domain: the canonical C2A domain (C2A wild type/C2A) and the variant resulting from alternative splicing of the first exon (C2Av1). Of the two C2 domains in cotton Syt I, only the C2A domain was studied. Purification of these constructs was carried out as previously described [4–6].

2.2. Preparation of lipid samples

All lipids were purchased from Avanti Polar Lipids (Birmingham, AL). Samples without cholesterol were prepared as previously described [6]. Cholesterol-containing samples were prepared by aliquoting lipid stocks into a 4:1 mixture of chloroform:methanol followed by rotary evaporation using a Buchi R-215 at a temperature between 50 and 60 °C. The lipid films were then placed under vacuum for a minimum of 8 h to remove excess solvent and hydrated with the appropriate buffer. LUVs were prepared by hand extrusion using a 0.1 μm filter. SUVs were prepared through multiple rounds of extrusion with filters of gradually smaller pore sizes ending with a 0.03 μm pore size. Lipid species used in the preparation of the LUVs included 1-palmitoyl-2-oleoyl-*sn*-glycero-3-phosphatidylcholine (16:0,18:1PC or POPC), 1-palmitoyl-2-oleoyl-*sn*-glycero-3-phosphatidylserine (16:0,18:1PS or POPS), as well as those shown in Table 1, including the various acyl chain compositions of phoshphatidylethanolamine (PE), phsophatidylinositol (PI), and phsophatidylserine (PS).

2.3. Differential scanning calorimetry (DSC)

DSC experiments as well as both scan rate and concentration dependent controls were performed on a NanoDSC (TA Instruments, New Castle, DE) as described previously [4–6]. All scans were conducted in chelexed 20 mM MOPS, and 100 mM KCl, pH 7.5 using saturating ligand concentrations. All scans with lipid contained one of the following: 1) LUVs of 60:40 POPC:POPS; 2) LUVs of (80:20):30 (POPC:POPS):cholesterol in which 30 mol% cholesterol was doped on top of a mixture of POPC:POPS (80:20); 3) LUVs with the mixture shown in Table 1 plus 45 mol% cholesterol doped in; or 4) SUVs composed of mixture 3. The concentration of the calcium stock solution used for all scans was verified using both a calcium ion selective electrode (ThermoScientific) and a BAPTA chelating assay (Invitrogen/Molecular Probes, Eugene, OR). The concentration of all lipid stock solutions was confirmed through a phosphate assay according to standard protocols [6]. For the experiments reported in this study the human Syt I C2A construct was found to have an average reversibility of 93% except in the presence of LUVs composed of the membrane domain forming mixture in which the reversibility was found to be 46%. For a comparison between consecutive denaturation scans, please see Supplementary data. For a justification of the thermodynamic parameters reported for the other domains discussed please see references [4–6].

2.4. Tryptophan fluorescence (TF)

TF experiments were performed on a Lifetime Spectrometer (Fluorescence Innovations, Bozeman, MT) using nanomolar protein concentrations as previously described [4,6]. No time-resolved measurements were made; instead the integrated intensity of the lifetime decay was used to monitor intrinsic tryptophan fluorescence (excitation and emission wavelengths of 295 and 340 nm, respectively). Buffers, Ca^{2+} stocks, and lipid samples used were identical to that described above in Section 2.3. Percent reversibility was measured by comparing the integrated fluorescence lifetime intensity of the sample before heating and after cooling. Due to the exceptionally low stability of the Dys and cotton Syt I C2A domains, no change in tryptophan fluorescence could be detected for these constructs. As a result, only the Syt I C2 domains were studied using this method.

Table 1
Phospholipid components in the membrane domain forming mixture (left columns), as well as the phospholipid components of the synaptic vesicle mimic mixture, where FA1 and FA2 represent the acyl chains attached to the glycerol backbone. These lipid compositions are based on those presented in [24], and are designed to capture the essence of the lipid diversity of the synaptic vesicle outer leaflet. The percentages listed for each phospholipid species represent the mole percent of that species within the total phospholipid mixture, while the percent given for cholesterol represents the mole percent found within the total mixture.

Membrane domain forming mixture				Synaptic vesicle mimic mixture			
	FA1	FA2	% Total phospholipid		FA1	FA2	% Total phospholipid
PE ratio							
3	16:0	18:1	38	3	16:0	18:1	38
2	18:0	18:1	25	2	18:0	18:1	25
1	18:0	22n6	13	1	18:0	22n6	13
PI ratio							
2	18:0	18:0	1	–	–	–	–
1	18:1	18:1	0.5	1	18:1	18:1	0.5
2	16:0	18:1	1	2	16:0	18:1	1
1	18:0	20:4	0.5	1	18:0	20:4	0.5
PS ratio							
3	16:0	16:0	7	–	–	–	–
1	18:0	22n6	2	1	18:0	22n6	12
2	18:0	18:1	5	2	18:0	18:1	10
3	16:0	18:1	7	–	–	–	–
Cholesterol	–	–	45%	Cholesterol	–	–	45%

2.5. Circular dichroism (CD)

CD experiments were performed on a Jasco CD Spectrometer (Annapolis, MD), using 15 μM of the Syt I C2A domain (residues 96–265) with 700 μM LUVs composed of POPC:POPS (60:40) and 1 mM Ca^{2+} in a 0.1 cm quartz cuvette. The spectrum was obtained in the same buffer system described in Sections 2.3 and 2.4. Data points were collected in 1 nm increments and averaged over 5 acquisitions. Spectra collected were corrected for any buffer contributions by subtracting a buffer scan from the corresponding protein scan.

2.6. Carboxyfluorescein (CF) release assay

LUVs containing carboxyfluorescein dye were prepared as previously described [6]. To determine the effect of protein binding on membrane leakage, the dye signal was monitored with excitation and emission wavelengths of 492 nm and 515 nm respectively as functions of time and temperature, upon the injection of ligand followed by the injection of protein to the sample. In the absence of ligand or protein, buffer composed of 20 mM MOPS, 100 mM KCl, and 0.02% NaN_3 was added to obtain constant increases of volume at each addition of solution. All fluorescence measurements were performed on a Fluorolog 3 double excitation and double emission monochromator (Horiba Jobin Yvon) in a 500 μL quartz cuvette. Appropriate temperatures were chosen to enhance membrane transition and perturbation of the LUV lipid compositions listed in Table 1, on which the experiments were performed [14]. Time and temperature dependent experiments were performed for a period of 60 min using a temperature controlled water bath (Pharmacia Biotech Multitemp III). The cuvette contained 300 μL of a liposome sample at the start of the fluorescence scan, 100 μL of buffer or Ca^{2+} solution titrated in after 15 min, and 85 μL of buffer or protein titrated in after 30 min. The cuvette was placed in the fluorometer and the scan was immediately started at constant temperature (20.4 °C). At the time of the second injection, the temperature was set to increase to 75 °C and the change in CF fluorescence was monitored in order to confirm consistency between experiments as well as dye release. Within the cuvette the concentration of the liposome was 200 μM and the concentration of the Ca^{2+} ion solution was 3 mM after its addition at 15 min. A 50.6 μM stock sample of the Syt I C2A domain (encoding residues 96–265) was added in one increment of 85 μL to obtain a concentration of 13.33 μM. Triton X-100 detergent was added after each scan to completely disrupt the membrane and confirm the presence of CF within the liposome as well as determine the maximum efflux.

3. Information theory for membranes

Information theory provides a means to study the amount of information contained within a data set [15]. Information theory applies to information content of a signal rather than its meaning. When we receive a signal, we receive information; meaning is what we then do with the signal after we receive it. Information is the uncertainty in the identity of the next signal; when the uncertainty of the next signal is high, then we gain a large amount of information. In contrast, if we are very certain of the identity of the next signal, then we gain little new information when it is received.

When applied within the context of a membrane surface, information theory could have the ability to quantify and predict a membrane's signaling potential. The information content of a variable is calculated in terms of informational entropy, which measures the predictability or uncertainty of that variable. A higher calculated entropy means a given variable is less certain, and therefore when it is detected (by us or by the molecule with which it interacts) a larger amount of information is transmitted [2]. The entropy $H(x)$ of any discrete variable within a distribution can be calculated in units of bits using:

$$H(x) = -\sum p(x_i) * \log_2(p(x_i)) \quad (1)$$

where $p(x_i)$ is the probability of event x occurring relative to all other events in the system such that the sum of all probabilities $p(x_i)$ equals 1 (*i.e.* $\sum p(x_i) = 1$). For example, when calculating entropy associated with the head group composition of a lipid surface $H(h)$, $p(h_i)$ represents the mole fraction of all lipids containing the ith type head group within the membrane composition. Similar calculations were made regarding the acyl chain composition and designated $H(a)$. Because a phospholipid is composed of both an acyl chain as well as a head group, the mole fraction of a given lipid within a membrane composition is the joint probability of its two independent variables such that $p(l) = p(h,a) = p(h) * p(a)$. Thus the entropy associated with a membrane's lipid composition is reported as the joint entropy $H(h,a)$ of its two variables. Continuing with the statistical nomenclature, $H(h)$ and $H(a)$ can then be described as marginal entropies of the joint lipid distribution. Several possible relationships between the joint entropy ($H(h,a)$) and marginal entropies ($H(a)$ and $H(h)$) of the system are described in Fig. 1.

In a system containing multiple randomly distributed variables, the marginal entropy of each variable is the uncertainty/information content contained within the composition of that variable and is independent of any other variable in the system. The joint entropy of the same system is the novel information content contained within the

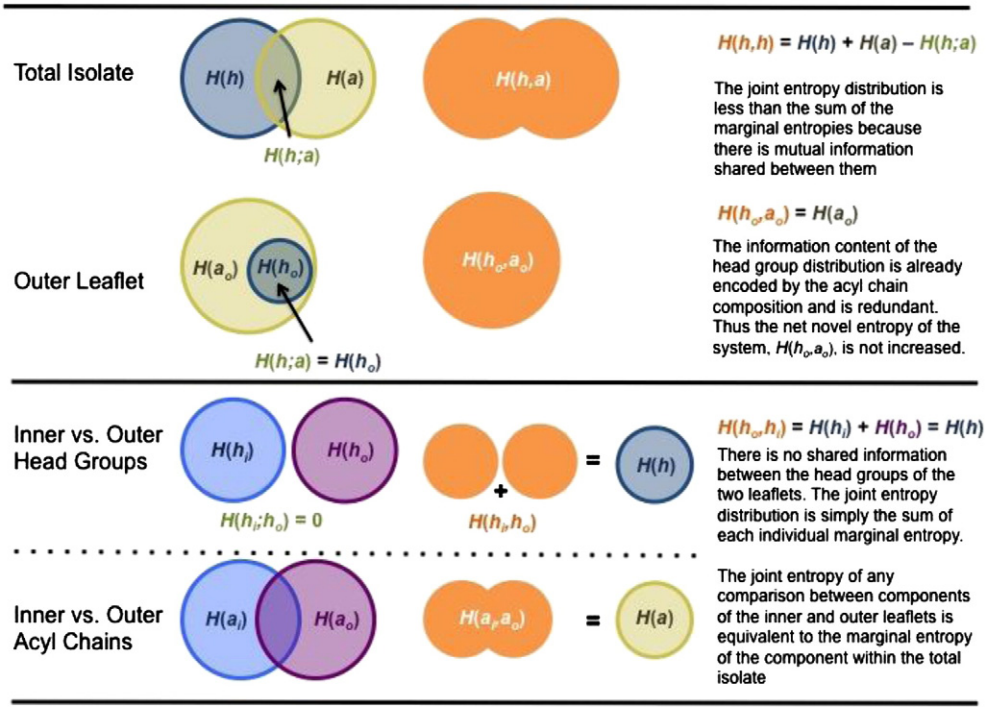

Fig. 1. Examples and explanations of the overlap of marginal entropies of variables within their joint entropy where the marginal entropy is $H(x)$, joint entropy is $H(x,y)$, and mutual information content is $H(x;y)$.

sum of the marginal entropies of all variables within the system (Fig. 1). The mutual information, $H(h;a)$, is the interdependence of two variables, and is the amount of common information content shared between the marginal entropies of the variables in the system. For instance, if you know that a particular acyl chain of a lipid in a given membrane composition associates with head groups with vastly different probabilities, knowing the acyl chain composition of a lipid automatically narrows the field of possibilities for the head group composition. In other words mutual information $H(h;a)$ is the amount of information you have automatically learned about one variable by knowing the other variable. (See Fig. 1 for a graphical explanation of the inter-relatedness of marginal entropy, joint entropy, and mutual information of various systems.)

Through the use of Eq. (1), by determining the mole fraction of each lipid component in a membrane, the marginal entropies $H(a)$ and $H(h)$, joint entropy $H(h,a)$, and mutual information content $H(h;a)$ of the lipid distribution can be calculated for both the relationship between the acyl chain and head group distributions, as well as the relationship between the information stored within and across both leaflets of the plasma membrane. Here we use the unit of a Bit as an absolute unit of measurement of the entropy/information content stored within the lipid composition of a membrane. Because it is calculated using the mole percentages of lipid species in the membrane it is independent of membrane or lipid concentration as long as membrane composition remains constant. In terms of the Shannon Information Index (Eq. (1)) the entropy of the system (calculated in bits) can be described as the predictability of a component on the membrane surface [15]. The lower the entropy of the lipid composition, the more easily the distribution of the lipid on the surface may be predicted. A higher entropy equates to a more random membrane composition and hence more information transferred by a particular realized state.

If it is assumed that the lipid composition of the entire membrane does not change over the course of a signaling event, upon domain formation the calculated entropy or information content of the entire membrane surface will remain the same. This is because the entropy of the membrane only depends on the membrane's lipid composition and not the lipid's physical distribution across the membrane surface. It is feasible, however, that due to a non-random distribution of lipids across the membrane surface, local regions of the membrane such as lipid rafts would have lower entropies due to the restriction of the lipid composition in those regions. This means that though the informational storage capacity of the membrane will remain the same if the relative ratios of lipids composing the membrane are constant, any event in which lipids are de-mixed would locally reduce entropy in the domains. In this way the joint entropy of a membrane can also be viewed as a unit of the maximum potential change that a local region of the membrane can undergo upon lipid de-mixing/domain formation. A membrane with 10 equally probable types of lipids undergoing domain formation to form localized domains which predominantly contain only 2 of the 10 different types of lipids underwent a larger local change in entropy than a membrane that underwent the same domain formation but only had 5 different types of lipids to begin with regardless of the fact that in both cases the entropy of the resultant domains would be the same. Thus a more complex membrane with higher entropy can induce larger changes in local membrane compositions which could allow for a discrete lipid signal to be either sensed or induced by membrane associated proteins above the level of random noise within a membrane's lipid distribution.

4. Results and discussion

4.1. Information content of a cell membrane surface

To determine the capacity of the membrane to encode information for signaling events, experimentally derived lipid compositions from the literature were analyzed using information theory. In the context of information theory we calculated the entropy (uncertainty) of various membrane isolates including the total lipid extract (TLE), plasma membrane blebs (PM), and detergent resistant extracts from either unstimulated (DRMu) or stimulated (DRMs) mast cells [13]. Each of the membrane isolates encodes between 5.6 and 5.8 bits of information in the joint distributions of their acyl chains and head groups (Table 2) with more information residing in the distribution of the acyl chains than in the distribution of the head groups.

Table 2
The information content or entropy (H) of membranes isolated from RBL-2H3 mast cells calculated in bits of information. Membrane samples included the total lipid extract (TLE), plasma membrane blebs (PM), and detergent resistant extracts of cells from both unstimulated (DRMu) and stimulated (DRMs) mast cells [13]. Information content was analyzed in terms of the total membrane isolate of each membrane sample as well as the information content of the inner and outer leaflets of the samples. DRM are detergent resistant membranes and correlate with membrane domain compatible lipid mixtures. Estimations of the 95% confidence intervals for the joint entropy calculations of each composition are shown with the exception of DRMs which lacked replicate analysis in the literature. Confidence intervals for other entropy calculations could not be completed due to constraints of the literature.

Bits of information	Total isolate				Outer leaflet			Inner leaflet		
	TLE	PM	DRMu	DRMs	PM	DRMu	DRMs	PM	DRMu	DRMs
Joint entropy: $H(h,a)$	5.6 ± 0.36	5.4 ± 0.18	5.7 ± 0.23	5.7 ± n/a	4.2 ± 0.15	4.0 ± 0.14	4.2 ± n/a	4.9 ± 0.11	5.1 ± 0.18	5.3 ± n/a
Marginal entropy head groups: $H(h)$	2.3	2.1	2.5	2.4	0.7	0.9	0.8	1.6	1.9	1.9
Marginal entropy acyl chains: $H(a)$	4.2	4.2	4.2	4.4	4.2	4.0	4.2	3.6	3.6	3.9
Mutual info. of head groups and acyl chains: $H(h;a)$	0.8	0.9	1.1	1.0	0.7	0.9	0.8	0.3	0.5	0.5
Mutual info. of leaflets: H (*outer*;*inner*)	–	3.8	3.4	3.7	–	–	–	–	–	–

To assess the relative information content of the inner and outer leaflets of the mast cell membrane, calculations were performed on each data set assuming an asymmetry of the bilayers in which the outer leaflet was composed mainly of sphingomyelin (SM) and PC head group-containing lipids while the inner leaflet contained an assortment of PE, PS, phosphatidylglycerol (PG), PI, and phosphatidic acid (PA) containing head groups [16,17]. The literature values used for the entropy calculations were tested against our assumption using geometric constraints based on the minimal curvature of the plasma membrane bilayer and the subsequent required parity of the number of molecules in each leaflet due to the hydrophobic effect. Our calculations indicate that PC and SM lipids represent 55% of the lipids in the bilayer, while the PE, PS, PG, PI, and PA lipids represent the remaining 45%, supporting (to a first approximation) our assumption of the bilayer asymmetry. We found that the joint entropy between the acyl chains and head groups of the inner leaflet of the membrane is approximately 1 bit higher than that of the outer leaflet (Table 2). For membrane associating proteins, this finding suggests that more information content is potentially presented to (and decoded by) those inside the cell than those outside the cell.

In addition to analyzing the joint entropy contained within the inner and outer leaflets of the membrane-isolates, the marginal entropies of the head groups and acyl chains within each leaflet were calculated. The inner leaflet contains higher entropy and more uncertainty in the head groups than the outer leaflet, while the outer leaflet contains more uncertainty in the acyl chains than the inner leaflet. Additionally, the marginal entropy of the head groups of the outer leaflet is entirely contained within the marginal entropy of its acyl chains. This implies that the PC and SM of the outer membrane have mutually exclusive subsets of acyl chains meaning the joint entropy of the system is entirely dependent on the acyl chain composition (Fig. 1). Knowing the acyl chain composition of a lipid in the outer leaflet of the PM determines the head group associated with it by default. This result is less surprising when considering the difference in the synthetic pathway of PC and SM, but might have interesting implications in the packing and distribution of the outer membrane.

When we calculated the information content of a mast cell's total plasma membrane extract as well as stimulated and non-stimulated detergent-resistant membrane extracts, we found that more information resided in the marginal entropy of the acyl chains than the head groups (Table 2). This is due in part, to the large degeneracy of acyl chain unsaturation. This was not solely a consequence of simply having a greater number of possible acyl chains than head groups, but because there are a greater number of significantly populated distinct chemical species and therefore more possible combinations in the former than the latter. Mass spectrometry is unable to resolve between each of the two acyl chains per phospholipid. Because of this the entropy of the system could be higher than what was calculated due to undercounting of the possible chemically distinct acyl chain combinations. Overall we found that the joint entropy between the acyl chains and head groups of the inner leaflet of the membrane is approximately 1 bit higher than that of the outer leaflet (Table 2). This increase is due, primarily, to the novel information content (*i.e.* non-zero conditional entropy) of the head group distribution of the inner leaflet. The mutual information $H(x;y)$ of two variables represents the redundant or shared information between the variable's marginal entropies (Fig. 1) and is a measure of the dependence of those two variables. In this way, the 3.4 to 3.8 bits of mutual information shared between the two leaflets of the membrane can be viewed as the extent of the interdependence of the bilayers.

Though the stimulation of the mast cells (DRMs) does not increase or decrease the joint entropy of the membrane isolates compared to the unstimulated (DRMu) it does increase the marginal entropies of the head groups, the acyl chains, and the mutual information shared between the two leaflets of the membrane isolates (Table 2). This result then, is consistent with the migration of polyunsaturated lipids into these detergent resistant membrane fractions resulting in increased shared information content between the domains, and a change in the distribution of information within the membrane. The higher information content of the inner leaflet, along with the changes in the information of the membrane brought upon by the redistribution of lipids through domain formation, presents the membrane as a highly responsive surface having the capacity to encode and propagate information.

4.2. C2 domains at neuronal, muscle, and plant membranes are weakly held together

C2 domains are functional modules exploited by numerous proteins in membrane trafficking and signaling events [18,19]. As such, they are likely candidates for the decoding and propagation of information stored within the membrane's changing lipid distribution as discussed above. Currently, there are 39 unique crystal structures of C2 domains that have been assigned *via* SCOP classification [20]. Of these structures most share a similar overall fold such as those in human synaptotagmin I, the canonical and variant forms of Dys, cytosolic phospholipase A_2 α, protein kinase C, and extended synaptotagmins (Fig. 2) [5,18,19,21]. No crystal structure is available for *Gossypium* (cotton) Syt I; however, a good quality homology model can be computed based on its similarity with human Syt I. While the C2 domain structures of human and cotton Syt I as well as the canonical and variant forms of Dys C2A are highly similar their free energies of stability at 37 °C ($\Delta G_{37\ °C}$) are not, spanning from 0.017 to 2.32 kcal/mol (Fig. 3, lower panels; Table 3). Despite this range, these different C2 domain stabilities are similar in the sense that all are at the lower limit of what constitutes a folded protein and all have features of protein disorder. Given that marginal stability is found in C2 domains from tissues of different embryonic origin (neurons and muscle) as well as different eukaryotic organisms (humans and plants), it poses the question of whether or not this is a conversed feature of membrane associated C2 domains. The initial data presented here suggests that this may be the case and earlier DSC denaturation work on the α-, β-, and γ-isoforms of protein kinase C, wherein all C2 domains were found to have a $\Delta G_{37\ °C}$ of ~1 kcal/mol, further supports this hypothesis [8].

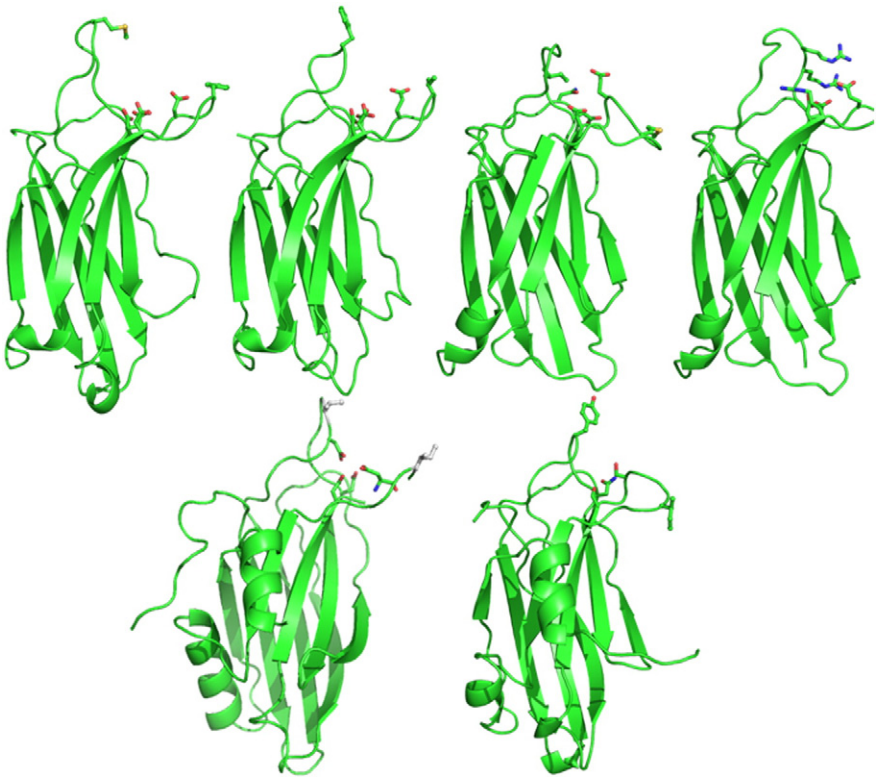

Fig. 2. Structures of various C2 domains. The top row of structures correspond to C2A domains (from left to right) of human Syt I, cotton Syt I, human canonical Dys, and human variant Dys. The bottom row of structures are C2B domains (from left to right) from human and cotton Syt I. The calcium binding residues are shown and the putative lipid interacting residues are in white balls-and-sticks. Note the high level of structural similarity.

4.3. Membrane composition and curvature set the protein ensemble

The marginal stability of the C2 domains tested above suggested that each would be sensitive to changes in their local environment, particularly the membrane surface (and encoded information content) with which they interact [22,23]. To test this hypothesis, a C2 domain construct of human Syt I was denatured in the presence of vesicles of varying lipid composition and the resulting data was used to calculate $\Delta G_{37\ ^\circ C}$. Human Syt I C2A (encoding residues 96–265) in the presence of non-domain forming LUVs (60:40 mixture of POPC:POPS) was found to be weakly stable with a $\Delta G_{37\ ^\circ C}$ of 2.18 kcal/mol (Fig. 3, upper left panel; Table 3). Such a membrane composition has a low information content as was determined using information theory as done above for mast cell membranes; the total stored information only amounts to 0.97 bits of information. When the composition includes cholesterol ((80:20):30 mixture of (POPC:POPS):chol as LUVs with an information content of 0.72 bits), this basal stability decreases to 1.67 kcal/mol (Fig. 4, middle panel; Table 3).

When the LUV membrane complexity mimics the heterogeneity of the plasma membrane (Table 1) and thus has greater information content (2.50 bits), C2A's stability and unfolding profile undergo additional dramatic changes (Fig. 4, middle panel). This plasma membrane mimic is based upon the distribution and mole percents of lipid species found in the cytosolic face of a synaptic vesicle with which Syt I interacts *in vivo* [24]. In the presence of this synaptic vesicle mimic and saturating Ca^{2+}, human Syt I C2A has a stability of 5.75 kcal/mol. If, however, physiological unsaturated PS and PI lipids are replaced with PS and PI containing saturated acyl chains, a chimeric lipid mixture is made; the composition of which still replicates the general characteristics and distributions found in a synaptic vesicle, but also weakly forms domains as suggested by the subtle DSC transition seen with LUVs alone (Fig. 4, left panel). Using this LUV chimera, the calculated $\Delta G_{37\ ^\circ C}$ in the presence saturating Ca^{2+} was 7.09 kcal/mol and increased further still to 7.6 kcal/mol using SUVs of identical composition. In the case of the chimera, the replacement of unsaturated PS and PI with saturated versions does not globally change the calculated information content of the membrane as discussed above. On a local level, however, the slight phase separation of saturated lipid would decrease information content allowing for a discrete phospholipid signal to be propagated above background membrane noise. Indeed, human Syt I C2A's $\Delta G_{37\ ^\circ C}$ increases 23% (5.75 to 7.09 kcal/mol) in response to this local change in lipid distribution and increases an additional 7% (7.09 to 7.6 kcal/mol) in response to the increased curvature. This latter observation is of particular importance to human Syt I because vesicles undergoing exocytosis and subsequent recycling experience a broad range of positive and negative curvatures both of which can change lipid distributions [25,26]. If Syt I senses these changes, as suggested by the change in $\Delta G_{37\ ^\circ C}$ presented here, it will have ramifications on the protein's conformational ensemble.

The same rule of membrane composition sensitivity seen for C2A alone seems to extend to the C2AB fragment of human Syt I, which includes both C2 domains of the protein [4]. The C2A and C2B domains are stabilized by different lipid species, where C2A is stabilized by phosphatidylserine (PS) and C2B by phosphatidylinositol (PIP_2) [4]. Because one domain becomes destabilized when the other is stabilized, both C2 domain ensembles are set by interactions with either lipid type. This is best illustrated in the TF denaturations of C2AB which have a strong fluorescence contribution from the C2B core tryptophan (Fig. 4, right panel). In the presence of 60:40 POPC:POPS LUVs, C2A is stabilized and C2B is destabilized (green). However, addition of Ca^{2+} drives C2A into a PS-bound state which makes the destabilization of C2B more prominent (orange and red). In contrast, when C2AB is in the presence of 95:5 POPC:PIP_2 LUVs, C2B is stabilized and C2A is destabilized (blue). As with a PS-containing membrane, Ca^{2+} accentuates this effect (purple). The denaturations reveal a strikingly broad range of stabilities that highlight the ability

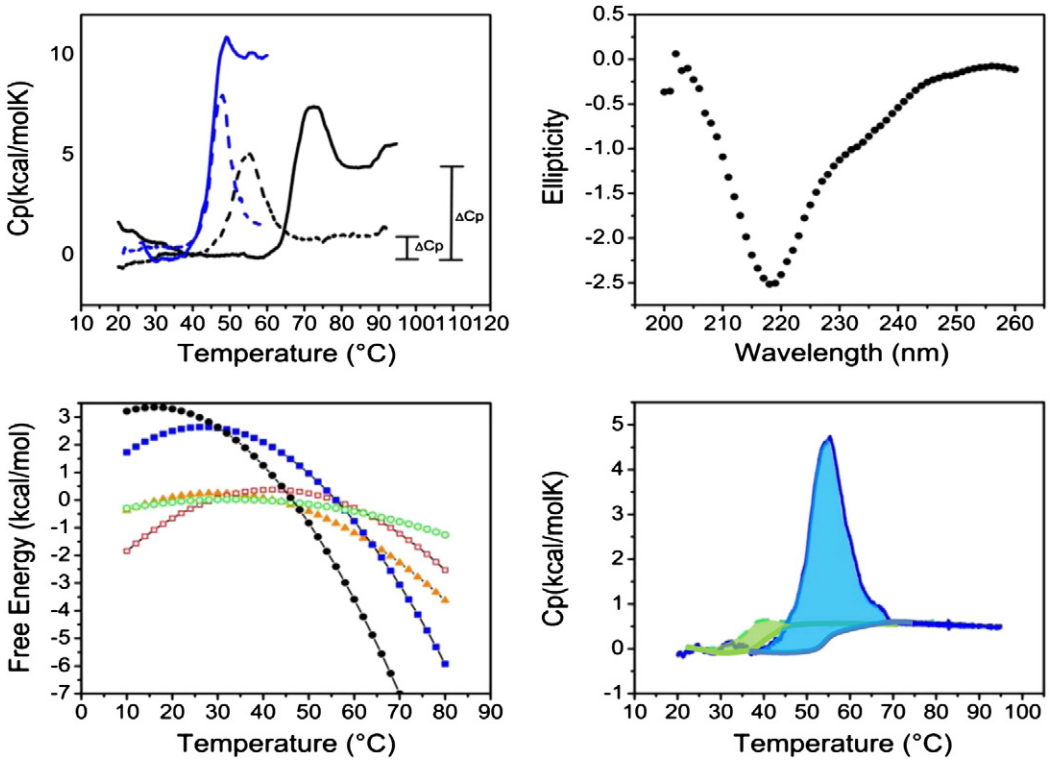

Fig. 3. *Upper panels*: The left panel shows the denaturation profile of human Syt I C2A (residues 96–265) at 13 μM in the presence of 1 mM LUVs composed of POPC:POPS (60:40) with either 1 mM EGTA (dashed line) or 1 mM Ca^{2+} (solid line). Also shown is 11 μM C2B in the presence of 490 μM LUVs composed of (95:5) POPC:PIP2 (solid blue line), 13 μM C2B in the presence of 0.5 mM EGTA (dashed blue line). The large ΔCp differences are highlighted for the C2A domain with brackets. The right panel is the CD spectrum obtained for human Syt I C2A (residues 96–265) in the presence of 700 μM LUVs composed of POPC:POPS (60:40) and 1 mM Ca^{2+}. *Lower panels*: The left panel shows the free energies of stability of several C2 domains, in the absence of ligand, over a range of temperatures. These stabilities were calculated through the use of the Gibbs–Hemholtz equation, utilizing the ΔH, ΔCp, and T_m obtained from the thermal denaturation profiles of the domains. The orange triangles, red squares, blue squares, green circles, and black circles represent canonical Dys C2A, Dys C2Av1, human Syt I C2A (residues 140–265), cotton Syt I C2A, and human Syt I C2B, respectively. The right panel compares the denaturation profile of the Syt I C2A domain of cotton (green, [Cotton C2A] = 175 μM) with that of the human Syt I C2A domain construct containing the amino acids 140–265 (blue; [Human C2A] = 13 μM) in the presence of 1 mM EGTA. The blue and green lines under the curves represent the baselines used for integration and the shaded regions under the curves represent the area which is the enthalpy of denaturation.

of the membrane to broaden or narrow the conformational ensemble of C2B within the C2AB fragment using the lipid binding ability of either domain. Just as in membrane domain formation, the narrowing C2 domain ensemble decreases information content and allows for the reception of a discrete message; however, the allosteric coupling that exists between C2A and C2B allows for further transformation of the initial membrane message. Allostery, in this case, enhances the inherent plasticity of C2 domains and their ability to coordinate membrane information [27].

The responsiveness of human Syt I C2 domains is further exemplified by a few peculiar changes in the baseline heat capacity (ΔC_p) (Fig. 3, top left panel). C2A and C2B have a very large ΔC_p under some membrane conditions. As can be seen in Table 3 the large ΔC_p values can have a dramatic effect on the calculated stability of the domain, as it narrows the temperature range over which the protein appears stable and consequently can give rise to a negative $\Delta G_{37\ °C}$. While we are not concluding that the C2A domain is unfolded under these conditions (indeed at 25 °C, a temperature well below

Table 3
Stability parameters obtained for C2 domains of Syt I and both isoforms of the C2A domain in dysferlin (Dys). The top portion of the table includes human Syt I and Dys data summarized from previous denaturation studies [4–6], as well as new measurements for cotton Syt I C2A. The parameters reported for the human Syt I C2A domain, in the top half of the table, were collected with the construct containing the amino acids 140–265. The lower portion of the table shows the stability parameters for the human Syt I C2A construct containing residues 96–265 in the presence of phospholipid bilayers of different compositions and size. All ΔG values reported represent free energy of stability at 37 °C.

	ΔH (kcal/mol)	ΔCp (kcal/mol·K)	T_m (°C)	$\Delta G_{37\ °C}$ (kcal/mol)	ΔS (kcal/mol·K)
Previously studied C2 domains in the absence of ligand					
Syt I C2A	58.7 ± 0.3	1.92 ± 0.09	55.99 ± 0.04	2.32 ± 0.05	0.178 ± 0.006
Syt I C2B	69.6 ± 0.6	2.19 ± 0.04	46.4 ± 0.1	1.74 ± 0.09	0.22 ± 0.01
Cotton Syt I C2A	2.5 ± 0.1	0.37 ± 0.09	39.5 ± 0.1	0.017 ± 0.01	0.008 ± 0.004
Dys C2A	12.6 ± 0.8	0.97 ± 0.01	42.2 ± 0.6	0.17 ± 0.02	0.040 ± 0.002
Dys C2Av1	18.3 ± 0.4	1.32 ± 0.01	55.6 ± 0.1	0.33 ± 0.02	0.058 ± 0.001
Human Syt I C2A (96–265) in the presence of lipid					
POPC:POPS (60:40)	59.2 ± 0.2	1.91 ± 0.04	53.32 ± 0.03	2.18 ± 0.02	0.181 ± 0.004
POPC:POPS (60:40) and Ca^{2+}	58.6 ± 0.4	4.50 ± 0.03	68.96 ± 0.06	−1.50 ± 0.01	0.171 ± 0.007
(POPC:POPS):cholesterol (80:20):30	67.9 ± 0.2	3.08 ± 0.02	68.04 ± 0.04	1.67 ± 0.01	0.199 ± 0.003
Membrane domain LUV and Ca^{2+}	135.7 ± 0.5	3.58 ± 0.01	68.6 ± 0.6	7.09 ± 0.06	0.413 ± 0.02
Membrane domain SUV and Ca^{2+}	140.8 ± 0.6	3.60 ± 0.02	75.3 ± 0.6	7.60 ± 0.02	0.429 ± 0.01
Synaptic mimic and Ca^{2+}	107.0 ± 0.1	2.75 ± 0.06	67.36 ± 0.01	5.75 ± 0.02	0.315 ± 0.001

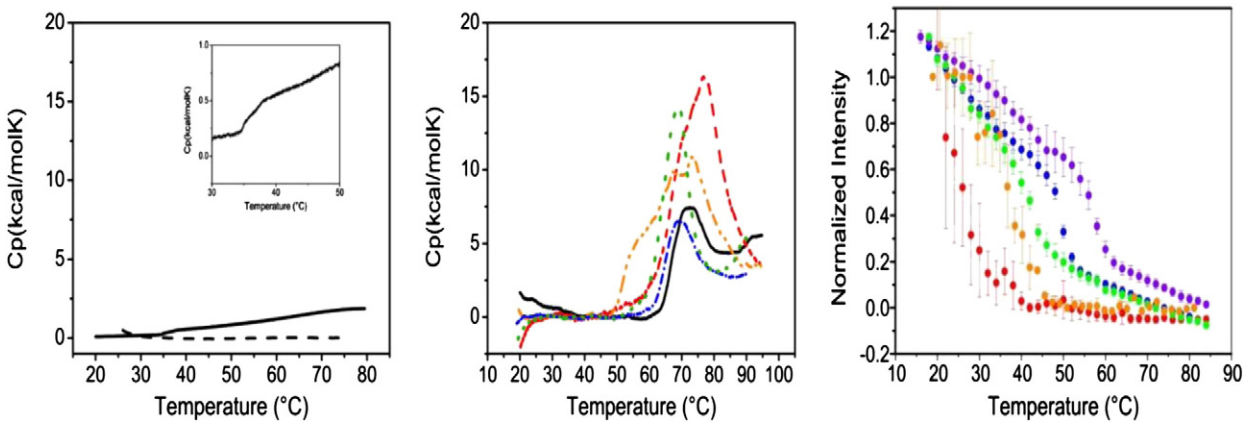

Fig. 4. *Left panel*: Thermograms obtained for LUVs of the membrane domain forming lipid mixture, at a phospholipid concentration of 3.3 mM (solid line) and the synaptic mimic mixture at a phospholipid concentration of 1 mM (dashed line). The inset in the upper right is a close-up of the phase transition. *Middle panel*: Denaturation profiles of 13 μM human Syt I C2A (residues 96–265) in the presence of 1 mM LUVs (unless stated otherwise) of different lipid compositions and 1 mM Ca^{2+}. The solid black line (▬) represents the denaturation with POPC:POPS (60:40); the blue dashed and dotted line (▬ · ▬ · ▬) represents the denaturation with (POPC:POPS):cholesterol (80:20):30; the yellow dashed and dotted line (▬ · · ▬) represents denaturation with the membrane domain forming lipid mixture from Table 1; the red dashed line (▬ ▬) represents the denaturation with the membrane domain forming lipid mixture as SUVs; and the green dotted line (· · ·) represents the denaturation with the synaptic vesicle mimic from Table 1. All DSC scans were conducted in a buffer composed of 20 mM MOPS and 100 mM KCl at a pH of 7.5. *Right panel*: TF denaturation of the C2AB fragment of Syt I in the presence of membrane with or without Ca^{2+}. Red: 0.75 μM C2AB, 5.1 mM Ca^{2+}, 110 μM LUVs (60:40, POPC:POPS). Orange: 0.9 μM C2AB, 600 μM Ca^{2+}, 1.2 mM LUVs (60:40, POPC:POPS). Green: 0.75 μM C2AB, 110 μM LUVs (60:40, POPC:POPS), 500 μM EGTA. Blue: 0.75 μM C2AB, 210 μM LUVs (95:5, POPC:PIP2), 500 μM EGTA. Purple: 0.75 μM C2AB, 5.1 mM Ca^{2+}, 210 μM LUVs (95:5, POPC:PIP2). Right panel adapted from [4].

the calculated cold denaturation threshold, C2A is still folded; Fig. 3 top right panel), the changes in ΔC_p provide another metric for the protein's sensitivity to the local membrane environment. Both C2 domains of human Syt I are known to have partial membrane insertion capabilities [28,29]. Moreover, structural orientation modeling of C2 domains bound to PIP_2 suggests a fairly large surface area of contact between protein and membrane [30]. Since one contribution to the change in baseline heat capacity is the change in solvation of the protein in native and denatured states, partial insertion into the 60:40 POPC:POPS (for C2A) or 95:5 POPC:PIP_2 (for C2B) membranes, or significant reduction in solvent accessibility due to surface adherence could alter solvation of the native C2 domain. If in the unfolded form of the protein, hydrophobic residues partially partitioned into the membrane, solvation could also be altered leading to a change in ΔC_p. This latter example however, would result in a reduced ΔC_p because hydrophobic residues would be protected from aqueous solution and not be surrounded by water cages that differentially absorb heat. Since this is the opposite of our data, the large ΔC_p's point instead to unique membrane modifications of the native state. Regardless of the root cause, the behavior of the C2 domain is membrane composition and condition-dependent.

4.4. Unique Syt I C2A conformers invoke distinct membrane-disruption responses in a synaptic vesicle mimic

From the cumulative denaturation studies above, it appears that these C2 domains (from human Syt I, in particular) are acutely sensitive to the membrane environment and are capable of adopting numerous conformations. This intrinsic plasticity leads to a question similar to that discussed for membrane lipid diversity and encoded information. Just as different lipid–lipid pairs constitute different potential signals, so too should C2 domain conformers. In this context, noise comes from the breadth of the C2 domain's conformational ensemble (determined by the free energy of stability). The signal is a particular subset of conformers that are simultaneously selected from the ensemble and more heavily weighted by the binding of ligand (such as membrane and Ca^{2+}). The resulting conformer subset mediates molecular events that fulfill a biological function of the C2 domain as a means to propagate the given signal [27].

To test this definition of function, we applied our recently developed carboxyfluorescein efflux assay to human Syt I C2A using vesicles that had either the domain forming or non-domain forming synaptic vesicle compositions listed in Table 1. From human Syt I C2A's change in stability shown above, it appears that the membrane domain forming mixture selects a smaller set of conformers from the ensemble (as suggested by the 23% increase in $\Delta G_{37\ °C}$ compared to the non-domain forming mixture). When looking at the change in efflux as a function of time, the C2A conformers selected by the domain forming mixture reduce release. This can be seen by the downward inflection at ~37 °C (where the phase transition occurs). However, when the lipid mixture mimics the synaptic vesicle, the extent to which C2A limits efflux increases; the downward inflection has a larger magnitude. In both cases though, when the sample temperature increases beyond the melting temperature of C2A, the rate of efflux increases dramatically. Thus the distinct C2A conformers selected by each lipid mixture send unique signals back to the membrane resulting in differential efflux outcomes that may relate to function (Fig. 5) [27].

5. Closing comments

Eukaryotic lipids are numerous. If each lipid combination is regarded as a potential signal, the eukaryotic membrane becomes a repository of information, highly diversified by chemical variation in head group and acyl chain. Indeed, when information content is calculated with information theory, it scales with lipid diversity as there are an increasing number of possible lipid–lipid combinations. These signals likely have specificity, suggested by both the unique lipid distributions found among compartments and leaflets as well as the numerous proteins that selectively bind to, partition into, or enzymatically target them. Within this context, a non-random distribution of lipids (like those found in membrane domains) could reduce information in a local region of the membrane. Membrane domains are non-ideal mixtures of lipids. As such, domains could have fewer potential combinations of lipids and consequently less information. This reduction of information can be conceptualized as an increase in the signal-to-noise ratio (S/N) of the membrane. The frequency of the lipid–lipid combination(s) that constitutes the domain (signal) increases at the expense of other lipid–lipid combinations (noise). In this scenario, predictable signaling outcomes come about from restricting available combinations of lipids either in a signaling domain or upon protein binding. While the DRM isolates of this study paradoxically showed an increase in information content,

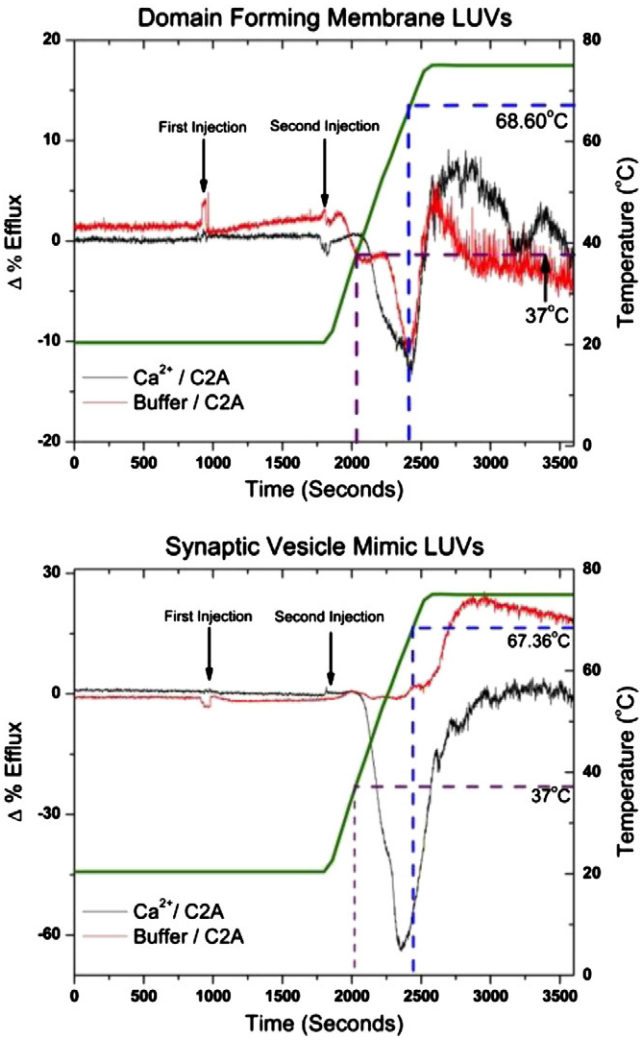

Fig. 5. Change in the percent efflux of carboxyfluorescein from 200 μM LUVs composed of a synaptic vesicle mimic lipid mixture (below) and LUVs composed of a domain forming lipid mixture (upper) injected with Ca^{2+} at 15 min and human Syt C2A domain (residues 96–265) at 30 min to final concentrations of 3 mM and 13.33 μM respectively. The change in the % efflux (Δ% efflux) was calculated by subtracting control titrations in which no protein was added during the second injection. Arrows indicate the addition of Ca^{2+} (1st injection), or protein (2nd injection) during the course of equilibration. For titration controls in which Ca^{2+} or protein were not present the injections were made with buffer composed of 20 mM MOPS, 100 mM KCl, and 0.02% NaN_3, pH of 7.5. For all titrations the temperature was held constant at 20.4 °C until equilibration of the second injection when it was set to increase to 75 °C. The green line represents the temperature change over time, while the blue and purple dashed lines represent the temperatures (and corresponding titration times) at which the membrane phase transition occurs (purple) and the bound-protein denatures (blue). The efflux conditions for both plots were as follows: the black solid line represents the Δ% efflux in the presence of both the human Syt C2A (residues 96–265) and Ca^{2+}, and the red represents the Δ% efflux of the domain in the absence of Ca^{2+}.

this likely resulted from detergent capture of multiple domains with varying lipid compositions, as the method of extraction cannot isolate one specific domain [31]. The information theory calculations, when applied to the much simpler 60:40 POPC:POPS mixture, indicate that indeed, fewer lipid components result in decreased information content (information content decreased from 5.6 bits in DRMs to 0.97 in 60:40 POPC:POPS mixture) consistent with domain formation being a means for increased lipid S/N.

Much like the membrane, C2 domains that associate with or are tethered to the membrane also seem to be dominated by weak interactions. This marginal stability imparts these proteins with a membrane-responsive character, where the conformational distribution of the protein is set by the lipid composition and information content. This selection/restriction of the protein conformational ensemble by the membrane can be viewed as a decrease in the informational entropy of the protein, which in turn reciprocally affects the membrane (Fig. 5). If lipid diversity is a means to store information (Table 2) and weakly stable membrane-associated proteins conformationally respond to membrane composition (Figs. 3 and 4) while simultaneously affecting membrane distribution (Fig. 5), then these weak interactions provide a means for translating and transducing membrane-encoded information to downstream effector molecules whether they be proteins required for membrane repair (Dys) or for regulated release of a neurotransmitter (human Syt I). In both cases, noise that manifests as non-functional combinations of lipids or non-functional protein conformers is unrecognized by the cell; the cell cannot make sense of the information presented in these non-signaling states. However, when a particular signal is to be transmitted, the near randomness of both lipid distribution and protein structure condenses into a particular configuration associated with the signal allowing for its propagation.

Acknowledgements

This material is based upon work supported by the National Science Foundation CAREER Award Grant Number (MCB-0845676). Any opinions, findings, and conclusions or recommendations expressed in this material are those of the authors and do not necessarily reflect the views of the National Science Foundation. Circular dichroism spectroscopy was performed at the Biophysical Spectroscopy Center at the University of Minnesota in Minneapolis.

Appendix A. Supplementary data

Supplementary data to this article can be found online at http://dx.doi.org/10.1016/j.bbamem.2014.03.005.

References

[1] P.F.F. Almeida, A. Pokorny, A. Hinderliter, Thermodynamics of membrane domains, Biochim. Biophys. Acta 1720 (2005) 1–13.
[2] H.J. Morowitz, Energy Flow in Biology, Ox Bow Press, 1968.
[3] V.J. Hilser, E.B. Thompson, Intrinsic disorder as a mechanism to optimize allosteric coupling in proteins, Proc. Natl. Acad. Sci. U. S. A. 104 (2007) 8311–8315.
[4] M.E. Fealey, J.W. Gauer, S.C. Kempka, K. Miller, K. Nayak, R.B. Sutton, A. Hinderliter, Negative coupling as a mechanism for signal propagation between C2 domains of synaptotagmin I, PLoS One 7 (e46748) (2012) 1–11.
[5] K. Fuson, A. Rice, R. Mahling, A. Snow, K. Nayak, P. Shanbhogue, A.G. Meyer, G.M.I. Redpath, A. Hinderliter, S.T. Cooper, R.B. Sutton, Alternate splicing of dysferlin C2A confers Ca(2+)-dependent and Ca(2+)-independent binding for membrane repair, Structure 104 (2013) 104–115.
[6] J.W. Gauer, R. Sisk, J.R. Murphy, H. Jacobson, R.B. Sutton, G.D. Gillispie, A. Hinderliter, Mechanism for calcium ion sensing by the C2A domain of synaptotagmin I, Biophys. J. 103 (2012) 238–246.
[7] I. Letunic, T. Doerks, P. Bork, SMART 7: recent updates to the protein domain annotation resource, Nucleic Acids Res. 40 (2011) D302–D305.
[8] A. Torrecillas, J. Laynez, M. Menéndez, S. Corbalán-García, J.C. Gómez-Fernández, Calorimetric study of the interaction of the C2 domains of classical protein kinase C isoenzymes with Ca^{2+} and phospholipids, Biochemistry 43 (2004) 11727–11739.
[9] J.W. Chen, P. Romero, V.N. Uversky, A.K. Dunker, Conservation of intrinsic disorder in protein domains and families: II. Functions of conserved disorder, J. Proteome Res. 5 (2006) 888–898.
[10] R.B. Gennis, Biomembranes: Molecular Structure and Function, 1st ed. Springer-Verlag, New York, NY, 1988.
[11] A. Hinderliter, P.F.F. Almeida, C.E. Creutz, R.L. Biltonen, Domain formation in a fluid mixed lipid bilayer modulated through binding of the C2 protein motif, Biochemistry 40 (2001) 4181–4191.
[12] A. Hinderliter, R.L. Biltonen, P.F. Almeida, Lipid modulation of protein-induced membrane domains as a mechanism for controlling signal transduction, Biochemistry 43 (2004) 7102–7110.
[13] E.K. Fridriksson, P.A. Shipkova, E.D. Sheets, D. Holowka, B. Baird, F.W. McLafferty, Quantitative analysis of phospholipids in functionally important membrane domains from RBL-2H3 mast cells using tandem high-resolution mass spectrometry, Biochemistry 38 (1999) 8056–8063.
[14] J.W. Gauer, K.J. Knutson, S.R. Jaworski, A.M. Rice, A.M. Rannikko, B.R. Lentz, A. Hinderliter, Membrane modulates affinity for calcium ion to create an apparent cooperative binding response by Annexin a5, Biophys. J. 104 (2013) 2437–2447.
[15] Claude E. Shannon, Warren Weaver, The Mathematical Theory of Communication, University of Illinois Press, 1971.

[16] M.S. Bretscher, Asymmetrical lipid bilayer structure for biological membranes, Nat. New Biol. 236 (1972) 11–12.
[17] J.A. Op den Kamp, Lipid asymmetry in membranes, Annu. Rev. Biochem. 48 (1979) 47–71.
[18] W. Cho, R.V. Stahelin, Membrane binding and subcellular targeting of C2 domains, Biochim. Biophys. Acta 1761 (2006) 838–849.
[19] J. Rizo, T.C. Südhof, C2-domains, structure and function of a universal Ca^{2+}-binding domain, J. Biol. Chem. 274 (1998) 15879–15882.
[20] H.M. Berman, J. Westbrook, Z. Feng, G. Gilliland, T.N. Bhat, H. Weissig, I.N. Shindyalov, P.E. Bourne, The Protein Data Bank, Nucleic Acids Res. 28 (2000) 235–242.
[21] J. Xu, T. Bacaj, A. Zhou, D.R. Tomchick, T.C. Südhof, J. Rizo, Structure and Ca^{2+}-binding properties of the tandem C2 domains of E-Syt2, Structure 22 (2014) 269–280.
[22] A. Bakan, I. Bahar, The intrinsic dynamics of enzymes plays a dominant role in determining the structural changes induced upon inhibitor binding, Proc. Natl. Acad. Sci. U. S. A. 106 (2009) 14349–14354.
[23] Y. Liu, I. Bahar, Sequence evolution correlates with structural dynamics, Mol. Biol. Evol. 29 (2012) 2253–2263.
[24] S. Takamori, M. Holt, K. Stenius, E.A. Lemke, M. Grønborg, D. Riedel, H. Urlaub, S. Schenck, B. Brügger, P. Ringler, S.A. Müller, B. Rammner, F. Gräter, J.S. Hub, B.L. De Groot, G. Mieskes, Y. Moriyama, J. Klingauf, H. Grubmüller, J. Heuser, F. Wieland, R. Jahn, Molecular anatomy of a trafficking organelle, Cell 127 (2006) 831–846.
[25] T. Brumm, The effect of increasing membrane curvature on the phase transition and mixing behavior of a dimyristol-sn-glycero-3-phosphatidylcholine/distearoyl-sn-glycero-3-phosphatidylcholine lipid mixture as studied by Fourier transform infrared spectroscopy and differential scanning calorimetry, Biophys. J. 70 (1996) 1373–1379.
[26] M.Ø. Jensen, O.G. Mouritsen, Lipids do influence protein function—the hydrophobic matching hypothesis revisited, Biochim. Biophys. Acta 1666 (2004) 205–226.
[27] M.E. Fealey, A. Hinderliter, Allostery and instability in the functional plasticity of synaptotagmin I, Commun. Integr. Biol. 6 (e22830) (2013) 1–4.
[28] A.A. Frazier, C.R. Roller, J.J. Havelka, A. Hinderliter, D.S. Cafiso, Membrane-bound orientation and position of the synaptotagmin I C2A domain by site-directed spin labeling, Biochemistry 42 (2003) 96–105.
[29] E. Rufener, A.A. Frazier, C.M. Wieser, A. Hinderliter, D.S. Cafiso, Membrane-bound orientation and position of the synaptotagmin C2B domain determined by site-directed spin labeling, Biochemistry 44 (2005) 18–28.
[30] J. Guillén, C. Ferrer-Orta, M. Buxaderas, D. Pérez-Sánchez, M. Guerrero-Valero, G. Luengo-Gil, J. Pous, P. Guerra, J.C. Gómez-Fernández, N. Verdaguer, S. Corbalán-García, Structural insights into the Ca^{2+} and PI(4,5)P2 binding modes of the C2 domains of rabphilin 3A and synaptotagmin 1, Proc. Natl. Acad. Sci. U. S. A. 110 (2013) 20503–20508.
[31] D.A. Brown, Lipid rafts, detergent-resistant membranes, and raft targeting signals, Physiology (Bethesda) 21 (2006) 430–439